ELSEVIER

EXPERIMENTAL HEMATOLOGY

Experimental Hematology 34 (2006) 1542–1552

Modification of glucocorticoid sensitivity by MAP kinase signaling pathways in glucocorticoid-induced T-cell apoptosis

Tomoko Tanaka[a,b], Taijiro Okabe[a], Shigeki Gondo[a], Mitsue Fukuda[c], Masahiro Yamamoto[c], Tsukuru Umemura[a], Kenzaburo Tani[b], Masatoshi Nomura[a], Kiminobu Goto[a], Toshihiko Yanase[a], and Hajime Nawata[a]

[a]*Department of Medicine and Bioregulatory Science, Graduate School of Medical Science;* [b]*Department of Molecular Genetics, Medical Institute of Bioregulation, Kyushu University, Fukuoka, Japan;* [c]*Clinical Research Institute, National Kyushu Medical Center Hospital, Fukuoka, Japan*

(Received 6 October 2005; revised 13 June 2006; accepted 27 June 2006)

Objective. **Glucocorticoid is widely used for the treatment of diseases such as hematological malignancies. Glucocorticoid sensitivity is different from person to person and the mechanism of the regulation of glucocorticoid sensitivity is not well known. Glucocorticoid resistance is a major clinical problem.**

Methods and Results. **Here, using glucocorticoid-induced T-cell apoptosis, a model system for the analysis of the mechanism of glucocorticoid action, we clarified that mitogen-activated protein kinases (MAPKs) modify glucocorticoid sensitivity, namely that the activation of extracellular signal–regulated protein kinase (ERK) and p38 MAP kinase reduce and enhance glucocorticoid sensitivity, respectively.**

Conclusion. **These findings might provide new tools for overcoming glucocorticoid-resistance.** © **2006 International Society for Experimental Hematology. Published by Elsevier Inc.**

Glucocorticoid is a stress hormone secreted from the adrenal gland. Glucocorticoid is physiologically involved in metabolism, cell differentiation, and several aspects of the maintenance of homeostasis. Pharmacologically, glucocorticoids have immunosuppressive, anti-inflammatory, and anti-allergic actions, and are administered for the treatment of diseases such as hematological malignancies and autoimmune diseases.

Glucocorticoid acts through glucocorticoid receptor (GR) to activate or repress the expression of target genes. Transcriptional regulation by GR depends on coregulators, such as coactivators and corepressors, modifying the chromatin structure or mediating the recruitment of the basic transcriptional machinery.

It has long been known that glucocorticoid induces apoptosis in thymocytes. In mice under stressful conditions, the thymus becomes involuted by thymocyte apoptosis. Glucocorticoid also induces apoptosis in T cell tumor cell lines derived from leukemia, lymphoma, or thymoma. Glucocorticoid-induced apoptosis in T cell tumor cell lines shares many common features with that in thymocytes.

Although functional GR is known to be required for glucocorticoid-induced apoptosis in T cells, it remains controversial as to which of the activation or repression functions of GR are involved in the apoptosis. A gene expression event is also known to be necessary for glucocorticoid-induced T-cell apoptosis from experiments using the RNA and protein synthesis blockers, actinomycin D and cycloheximide, respectively. In any case, enhanced expression of pro-apoptotic genes or inhibited expression of anti-apoptotic genes could be necessary for glucocorticoid-induced T-cell apoptosis, although the target genes remain to be elucidated [1–4].

It is generally thought that glucocorticoid-induced T-cell apoptosis is performed through a mitochondrial pathway [1–4]. Apoptosis through mitochondria is regulated by *bcl*-2 family members, which include *bcl*-2, *bcl*-xL, Bak, Bax, Bad, and Bim. *bcl*-2 and *bcl*-xL are anti-apoptotic, while Bak, Bax, Bad, and Bim are pro-apoptotic [5,6]. After the apoptotic signal reaches the mitochondria, several factors are released from the intermembrane space, leading to the activation of caspases and relief of the inhibitory activity of inhibitors of apoptosis proteins (IAPs) against caspases. These signals cause several apoptotic phenotypes

Offprint requests to: Taijiro Okabe, M.D., Ph.D., Department of Medicine and Bioregulatory Science, Graduate School of Medical Science, Kyushu University, Maidashi 3-1-1, Higashi-ku, Fukuoka, 812-8582 Japan; E-mail: tokabe@intmed3.med.kyushu-u.ac.jp

0301-472X/06 $–see front matter.
doi: 10.1016/j.exphem.2006.06.018

including externalization of phosphatidylserine, chromatin condensation, and DNA fragmentation [7,8].

There are at least four distinct groups of mitogen-activated protein kinases (MAPK): the extracellular signal–regulated protein kinases (ERK), the p38 MAP kinases, the c-Jun NH_2-terminal kinases (JNK), and ERK5, also referred to as BMK-1 [9,10]. MAPKs have been shown to be involved in numerous biological phenomena including cell survival and cell death. It is generally thought that ERK is involved in cell proliferation and survival, while on the other hand, p38 and JNK are involved in stress response and apoptosis, although the response depends on the cell type and the surrounding context (Fig. 1) [11,12]. ERK5, the least studied MAPK, is activated by a variety of growth factors and stress stimuli [10]. MAPKs are activated by a series of phosphorylation cascades, the so-called MAPK phosphorelay module, consisting of MAP kinase kinase kinase (MAPKKK), MAP kinase kinase (MAPKK), and MAPK. MAPKKK, activated by several stimuli, phosphorylates and activates MAPKK, and then activated MAPKK phosphorylates and activates MAPK. MAPK, in turn, phosphorylates and activates several substrates including other protein kinases and transcription factors. MAPKK is a dual-specificity kinase phosphorylating both a threonine and a tyrosine residue in the activation loop of MAPK to activate it [13,14].

To examine the cross-talk between glucocorticoid and MAPK signaling pathways in glucocorticoid-induced T-cell apoptosis, the effects of inhibition or activation of the MAPK phosphorelay module were investigated at several steps of apoptosis in a T cell leukemia cell line, CCRF-CEM.

Results

Dexamethasone-sensitive cell line CC7 and dexamethasone-resistant cell line CC3

In the human T lymphoblast cell line CCRF-CEM, apoptosis can be induced by a synthetic glucocorticoid, dexamethasone. It has been reported that CCRF-CEM cells are heterogeneous and contain both dexamethasone-sensitive and dexamethasone-resistant populations [15,16]. We subcloned several dexamethasone-sensitive and dexamethasone-resistant cell lines using the limiting-dilution technique, and analyzed the externalization of phosphatidylserine by annexin V binding. In the most sensitive clone, named CC7, after treatment with 10^{-6} M dexamethasone for 48 hours, the percentage of annexin V binding–positive cells was 51.2% ± 2.96% and the majority of annexin V binding–positive cells were negative for the uptake of propidium iodide (PI) dye. On the other hand, in the most resistant clone, named CC3, after the same treatment with dexamethasone, only a small percentage of cells were positive for annexin V binding (Fig. 1).

In order to investigate the dose dependency of dexamethasone, CC7 cells were untreated, or treated with 10^{-8} M, 10^{-7} M, or 10^{-6} M dexamethasone. As a result, 8.50% ± 0.20%, 8.58% ± 0.52%, 35.2% ± 1.05%, and 51.2% ± 2.96% of cells became positive for annexin V binding, respectively, showing that dexamethasone induced annexin V binding in a dose-dependent manner (Fig. 2A). On the other hand, only a small percentage of CC3 cells became positive for annexin V binding at each concentration of dexamethasone (Fig. 2B).

To delineate the effects of MAP kinase inhibitors on glucocorticoid-induced apoptosis, the externalization of phosphatidylserine was analyzed by annexin V binding in the presence or absence of dexamethasone with or without U0126, an ERK inhibitor, or SB203580, a p38 inhibitor.

In the presence of 10 μM U0126, after treatment with 10^{-8} M, 10^{-7} M, or 10^{-6} M dexamethasone, 18.8% ± 1.40%, 83.6% ± 2.72%, and 93.6% ± 2.02% of cells were positive for annexin V binding, respectively. U0126 alone had no effect on the annexin V binding (Fig. 2A), suggesting that ERK may inhibit glucocorticoid-induced T-cell apoptosis. In order to investigate the dose dependency of U0126, CC7 cells were untreated, or treated with 0.1 μM, 1 μM, or 10 μM U0126 in the presence of 10^{-7} M dexamethasone. As a result, 37.3% ± 3.88%, 42.0% ± 2.42%, 83.5% ± 1.27%, and 91.0% ± 1.41%

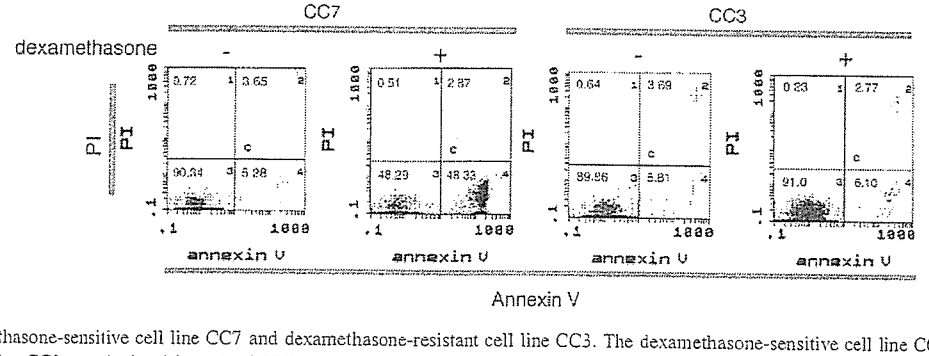

Figure 1. Dexamethasone-sensitive cell line CC7 and dexamethasone-resistant cell line CC3. The dexamethasone-sensitive cell line CC7 and dexamethasone-resistant cell line CC3 were isolated from the CCRF-CEM cell line. Both CC7 cells and CC3 cells were cultured for 48 hours in the presence or absence of 10^{-6} M dexamethasone, and tested for the externalization of phosphatidylserine by annexin V binding using a flow cytometer. The dot plots represent one of three independent experiments.

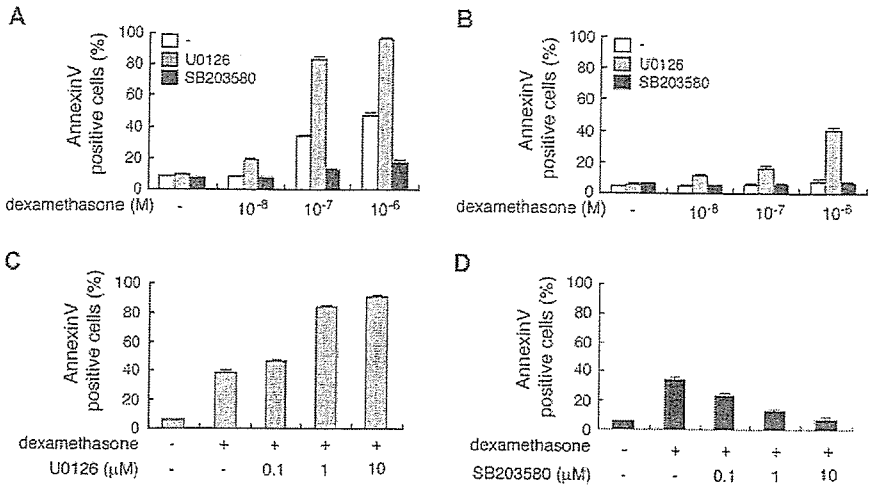

Figure 2. The effects of the MAPK inhibitors on the externalization of phosphatidylserine. Dexamethasone-sensitive CC7 cells (**A**) and dexamethasone-resistant CC3 cells (**B**) were cultured for 48 hours with different concentrations of dexamethasone in the presence or absence of 10 μM U0126 or 10 μM SB203580. Externalization of phosphatidylserine was detected by annexin V binding, and the percentage of annexin V–binding cells was calculated. White, gray, and black bars indicate no treatment, and treatments with 10 μM U0126 and 10 μM SB203580, respectively. To test the dose dependency, CC7 cells were cultured for 48 hours with different concentrations of U0126 (**C**) or SB203580 (**D**) in the presence or absence of 10^{-7} M dexamethasone. The data are the mean ± SE of three independent experiments.

of cells became positive for annexin V binding, respectively, showing that U0126 enhanced the action of dexamethasone in a dose-dependent manner (Fig. 2C).

On the other hand, in the presence of 10 μM SB203580, after treatment with 10^{-8} M, 10^{-7} M, or 10^{-6} M dexamethasone, 7.50% ± 0.20%, 12.0% ± 0.92%, and 15.6% ± 2.52% of cells were positive for annexin V binding, respectively. SB203580 alone had no effect on the annexin V binding (Fig. 2A), suggesting that p38 may enhance glucocorticoid-induced T-cell apoptosis. In other words, p38 may be necessary for glucocorticoid-induced T-cell apoptosis. In order to investigate the dose dependency of SB203580, CC7 cells were untreated, or treated with 0.1 μM, 1 μM, or 10 μM SB203580 in the presence of 10^{-7} M dexamethasone. As a result, 35.2% ± 2.22%, 23.5% ± 1.87%, 14.3% ± 0.81%, and 7.27% ± 1.92% of cells became positive for annexin V binding, respectively, showing that SB203580 inhibited the action of dexamethasone in a dose-dependent manner (Fig. 2D).

Next, dexamethasone-resistant CC3 cells were untreated, or treated with 10^{-8} M, 10^{-7} M, or 10^{-6} M dexamethasone in the presence of 10 μM U0126. As a result, 6.1% ± 1.39%, 11.6% ± 1.48%, 15.9% ± 2.31%, and 40.9% ± 1.76% of cells became positive for annexin V binding, respectively (Fig. 2B), suggesting that suppression of the activation pathway of ERK may make glucocorticoid-resistant cells glucocorticoid sensitive.

Effects of U0126 and SB203580 on several steps of apoptosis

Next, the effects of U0126 and SB203580 on several steps of apoptosis, including the mitochondrial membrane potential, caspase-3-like activity, DNA fragmentation, and chromatin condensation, were analyzed in CC7 cells.

First, we analyzed the loss of mitochondrial membrane potential using the fluorescent probes JC-1 and $DiOC_6$. JC-1 has been shown to be specific for measuring changes in the mitochondrial membrane potential. Loss of the mitochondrial membrane potential is indicated by a shift in the fluorescence from red to green [17]. In Figure 3A, the outlined region 1 (R1) and region 2 (R2) indicate J aggregates (red fluorescence) and JC-1 monomers (green fluorescence), respectively. The percentage of the R2 population was 6.2% and 49.0% in the absence or presence of 10^{-6} M dexamethasone for 48 hours, respectively. This increase in the R2 population induced by dexamethasone was enhanced by U0126 (R2; 87.4%) and inhibited by SB203580 (R2; 12.2%). U0126 or SB203580 alone had little effect on the R1 and R2 populations. In the presence of U0126, there was a small decrease in the red fluorescence of R1 in either the presence or absence of dexamethasone. The meaning of this phenomenon is not clear.

Figure 3A also shows the results of the analysis using the other fluorescent probe, $DiOC_6$. Both PI-negative and $DiOC_6$-positive cells were in the normal mitochondrial membrane potential state. Treatment with dexamethasone resulted in a decrease in the intensity of $DiOC_6$. The low-intensity population of $DiOC_6$ in the presence of dexamethasone (42.7%) was enhanced by U0126 (93.9%), and inhibited by SB203580 (8.9%). U0126 or SB203580 alone had little effect on the mitochondrial membrane potential.

Activated caspase-3 was then measured using anti-active caspase-3 antibody as described in the experimental

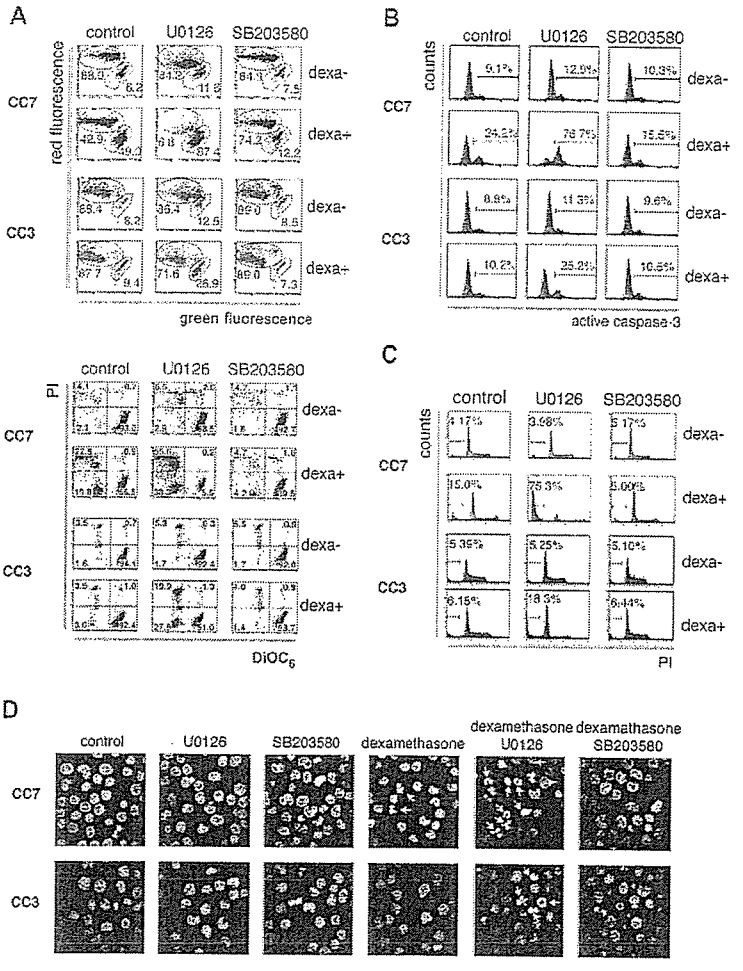

Figure 3. Effects of U0126 and SB203580 on several steps of apoptosis. Both CC7 cells and CC3 cells were cultured for 48 hours with or without dexamethasone in the presence or absence of 10 μM U0126 or 10 μM SB203580. The concentration of dexamethasone was 10^{-6} M unless described. **(A)** Loss of mitochondrial membrane potential was detected with the cationic fluorescence probes JC-1 and $DiOC_6$. **(B)** Caspase-3 activity was analyzed with anti-active caspase-3 antibody. The number in each histogram indicates the percentage of cells containing activated caspase-3. **(C)** DNA fragmentation was detected with PI using a flow cytometer. The percentage of the sub-G_0/G_1 fraction was calculated as described in the Materials and methods, and is shown in each histogram. **(D)** Nuclear morphology was observed with Hoechst 33342 staining under a confocal microscope. White arrows show apoptotic cells. The dot plots, histograms, and micrographs represent one of three independent experiments.

procedures. Caspase-3 activity was represented by an increase in the phycoerythrin fluorescence intensity.

As shown in Figure 3B, the population of cells containing activated caspase-3 increased from 9.1% to 24.2% after treatment with 10^{-7} M dexamethasone for 48 hours. Concomitant use of 10 μM U0126 or SB203580 changed the population of cells containing activated caspase-3 to 76.7% and 15.5%, respectively. U0126 or SB203580 alone had little effect on the caspase-3-like activity.

DNA fragmentation was then analyzed. Apoptotic cells containing fragmented DNA were represented by the so-called sub-G_0/G_1 population in the cell-cycle analysis using PI. As shown in Figure 3C, the sub-G_0/G_1 population increased from 4.17% to 15.0% after treatment with 10^{-6} M dexamethasone for 48 hours. Concomitant use of 10 μM U0126 or SB203580 changed the sub-G_0/G_1 population to 75.3% and 5.00%, respectively. U0126 or SB203580 alone had little effect on the sub-G_0/G_1 population.

As another apoptotic change in the nucleus in addition to DNA fragmentation, chromatin condensation was also analyzed. Chromatin condensation was actually induced by treatment with dexamethasone, and concomitant use of U0126 or SB203580 augmented or inhibited it, respectively (Fig. 3D).

The above data showed that U0126 enhanced and SB203580 inhibited dexamethasone-induced apoptosis during several steps of apoptosis including the externalization of phosphatidylserine, loss of mitochondrial membrane potential, caspase-3 activity, DNA fragmentation, and chromatin condensation in CC7 cells, supporting the idea that ERK inhibits and p38 enhances glucocorticoid-induced T-cell apoptosis. These data also suggest that ERK and

p38 affect the apoptosis process at the premitochondrial or mitochondrial stage.

The effect of U0126 on the several steps of apoptosis described above was also investigated in CC3 cells. First, in the loss of mitochondrial membrane potential using the fluorescent probe JC-1, the percentage of the R2 population in the presence of 10^{-6} M dexamethasone for 48 hours was increased by U0126 from 9.4% to 26.9%. In the loss of mitochondrial membrane potential using the other fluorescent probes $DiOC_6$, the low-intensity population of $DiOC_6$ in the presence of dexamethasone was increased by U0126 from 6.5% to 47.8% (Fig. 3A). The population of cells containing activated caspase-3 in the presence of 10^{-7} M dexamethasone for 48 hours was increased from 10.2% to 25.2% by the concomitant use of 10 μM U0126 (Fig. 3B). As for DNA fragmentation, apoptotic cells in the sub-G_0/G_1 population in the cell-cycle analysis using PI in the presence of 10^{-6} M dexamethasone for 48 hours ware increased by the treatment of 10 μM U0126 from 6.15% to 18.3% (Fig. 3C). Chromatin condensation was induced by the concomitant use of dexamethasone and U0126 (Fig. 3D). These results suggest that the treatment of U0126 relieves glucocorticoid resistance in CC3 cells at the premitochondrial or mitochondrial stage.

To directly demonstrate the hypothesis that ERK inhibits and p38 enhances glucocorticoid-induced T-cell apoptosis, the effects of transient expression of constitutive-active MEK1 or MKK6 were investigated. The low transfection efficiency in T cells made it difficult to analyze the effects of gene expression product by transient transfection. Nucleofector (Amaxa Biosystems, Cologne, Germany) dramatically improved the transfection efficiency. The proportion of cells expressing more than 10-fold the GFP fluorescence after transfection of pEGFP-C1, an EGFP expression vector, was 7.8% ± 2.8% (mean ± SD) (Fig. 4A). Transfection of the expression vectors for constitutive-active MEK1 (pFC-MEK1) or MKK6 (pcDNA3.1-MKK6 SETE) with pEGFP-C1 at a concentration ratio of 4 to 1 ensured the expression of MEK1 or MKK6 in the GFP-expressing cells. Cells transfected with the control vector pcDNA3.1 and pEGFP-C1 at a concentration ratio of 4 to 1 were incubated in the absence or presence of dexamethasone, and the cells expressing more than 10-fold the GFP fluorescence were sorted and analyzed for annexin V binding. Treatment with dexamethasone increased the population of annexin V–binding cells from 3.5% to 30.6% (Fig. 4B). In a similar manner, the expression vectors for constitutive-active MEK1 or MKK6 were transfected with pEGFP-C1. In cells expressing constitutive-active MEK1 or MKK6, 20.9% and 54.3% of cells were positive for annexin V binding, respectively, in the presence of dexamethasone (Fig. 4B). Since U0126 also inhibits ERK5 at higher concentrations, the effect of constitutive-active form of MEK5, a direct activator of ERK5, was also investigated. In cells expressing constitutive-active MEK5 or a control expression vector, 35.8% and 38.9% of cells were positive for annexin V binding, respectively (Fig. 4B). These data from the overexpression study suggest that ERK (ERK1/2) inhibits and p38 enhances glucocorticoid-induced T-cell apoptosis, and that ERK5 shows little effect if any.

In order to investigate the effect of knocking down ERK or p38, CC7 cells were transfected with siRNA for ERK1/2 or p38α/β or FAM-labeled control siRNA by Nucleofector. Since SB203580 inhibits both p38α and p38β among P38 isoforms, the inhibition of p38 by SB203580 is considered to be through p38α/β. Almost all cells transfected with FAM-labeled control siRNA showed FAM fluorescence; the transfection efficiency of siRNAs into CC7 cells was considered to be near 100%.

The mRNA levels of ERK1/ERK2 or p38α/p38β in CC7 cells transfected with siRNA for ERK1/2 or p38α/β, respectively, was analyzed by real-time PCR. Given the mRNA level for the control siRNA 1.0, the relative mRNA levels of ERK1, ERK2, p38α, and p38β were 0.13, 0.12, 0.54, and 0.17, respectively (Fig. 4C).

Treatment with dexamethasone increased the population of annexin V binding–positive cells from 5.5% to 58.8% in cells transfected with control siRNA. In cells transfected with ERK1/2 or p38α/β, 67.5% and 49.2% of cells were positive for Annexin V binding, respectively, in the presence of dexamethasone. In the absence of dexamethasone, siRNA for ERK1/2 or p38α/β showed no effect on annexin V binding, respectively (Fig. 4D).

These data show that knocking down ERK1/2 or p38α/β enhances or inhibits glucocorticoid-induced T-cell apoptosis, respectively.

Analysis of the effect of ERK or p38 on the transactivation or transrepression function of GR

Next, the effects of the activation of ERK or p38 on the transactivation or transrepression function of GR were investigated. First, the transactivation function of GR was analyzed using both $(GRE)_2$-tk-luc and MMTV-luc as reporter plasmids. In cells transfected with the control vector and $(GRE)_2$-tk-luc, dexamethasone treatment increased the relative luciferase activity from 0.01 ± 0.002 to 0.05 ± 0.003. Transfection with the expression vectors for constitutive-active MEK1, MKK3, or MKK6 increased the luciferase activity to 0.10 ± 0.015, 0.08 ± 0.023, and 0.08 ± 0.011, respectively, in the presence of dexamethasone (Fig. 5A). Then, MMTV-luc was used as a reporter plasmid, and similar experiments were performed. In the cells transfected with the control vector or the expression vectors for constitutive-active MEK1, MKK3, or MKK6 in the presence of dexamethasone, the relative luciferase activity was 0.17 ± 0.005, 0.15 ± 0.005, 0.17 ± 0.010, and 0.17 ± 0.008, respectively. In the untreated cells, the luciferase activity was nearly at the background level (Fig. 5B). These data suggest that both ERK and p38 either activate or do not change the GR transactivation function, depending on the target genes.

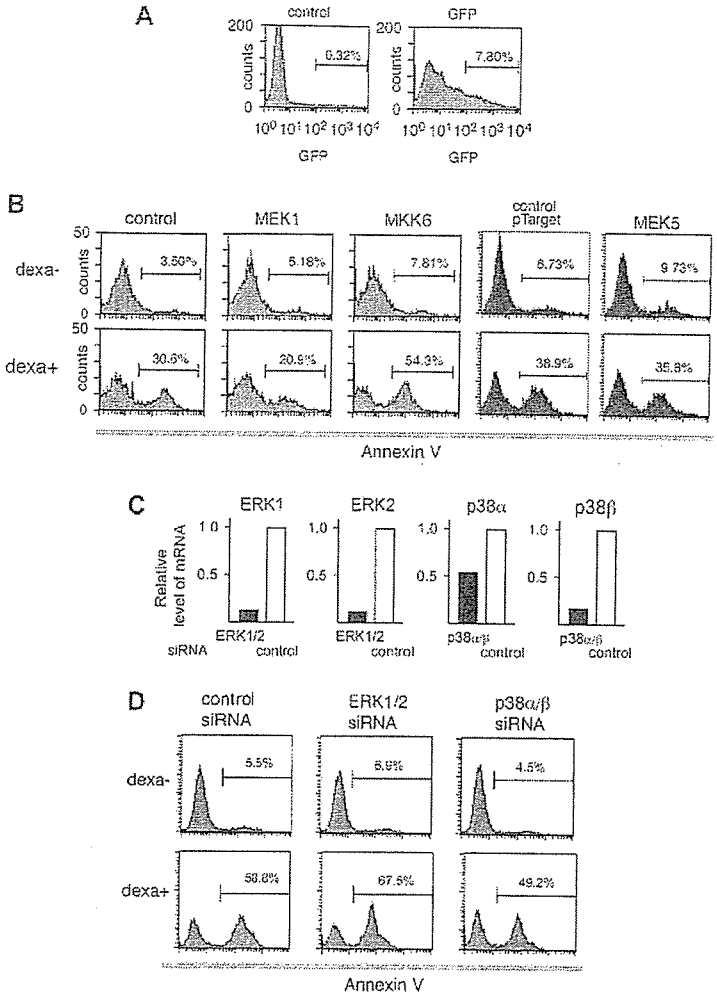

Figure 4. The effects of activation or inhibition of MAP kinase pathways on the externalization of phosphatidylserine. 5 × 10^6 CC7 cells were transfected with 1 μg of pEGFP-C1 and 4 μg of either a vector plasmid encoding constitutive-active MEK1, MKK6, or MEK5 and a control expression vector, and treated with or without 10^{-6} M dexamethasone for 40 hours. The cells exhibiting more than 10-fold of GFP fluorescence were sorted (**A**) and analyzed for annexin V binding (**B**). The number in each histogram in (**B**) indicates the percentage of annexin V–binding cells. (**C,D**) CC7 cells were transfected with siRNA for ERK1/2, p38α/β, or control siRNA and cultured for 48 hours. The comparative mRNA level for ERK1, ERK2, p38α, and p38β was calculated with quantitative real-time PCR method, respectively (**C**). The ratio of annexin V–positive CC7 cells, in which mRNA level of ERK1/2 or p38α/β was downregulated by siRNA, was analyzed (**D**). The dot plots and histograms represent one of three independent experiments. The histograms represent one of three independent experiments.

Then, the transrepression function of GR was investigated by analyzing the degree of repression of TNF-α-activated nuclear factor-κB (NF-κB) activity by dexamethasone. The luciferase activity in the absence of TNF-α in cells transfected with the control vector was set as 1. In the control cells, dexamethasone suppressed the TNF-α-activated NF-κB activity from 9.8 ± 1.5 to 4.4 ± 1.6. In cells transfected with the expression vectors for the constitutive-active MEK1, MKK3, or MKK6, dexamethasone treatment suppressed the TNF-α-activated NF-κB activity from 8.5 ± 1.5, 10.6 ± 2.3, and 10.3 ± 1.7 to 4.0 ± 1.3, 4.3 ± 1.6, and 4.5 ± 0.4, respectively (Fig. 5C). These data suggested that neither ERK nor p38 has any effect on transrepression function of GR. The results of the effects of ERK and p38 on the transactivation or transrepression function of GR could not explain the opposite effects of ERK and p38 on glucocorticoid-induced T-cell apoptosis, suggesting that the main target of ERK and p38 in glucocorticoid-induced T-cell apoptosis is not the level of transcription regulated by GR, although this possibility cannot be excluded.

Analysis of the steady-state protein expression levels of bcl-2 and IAP family members

As described before, apoptosis through mitochondria is regulated by *bcl*-2 family members, which consist of both anti-apoptotic members, such as *bcl*-2 and *bcl*-xL, and

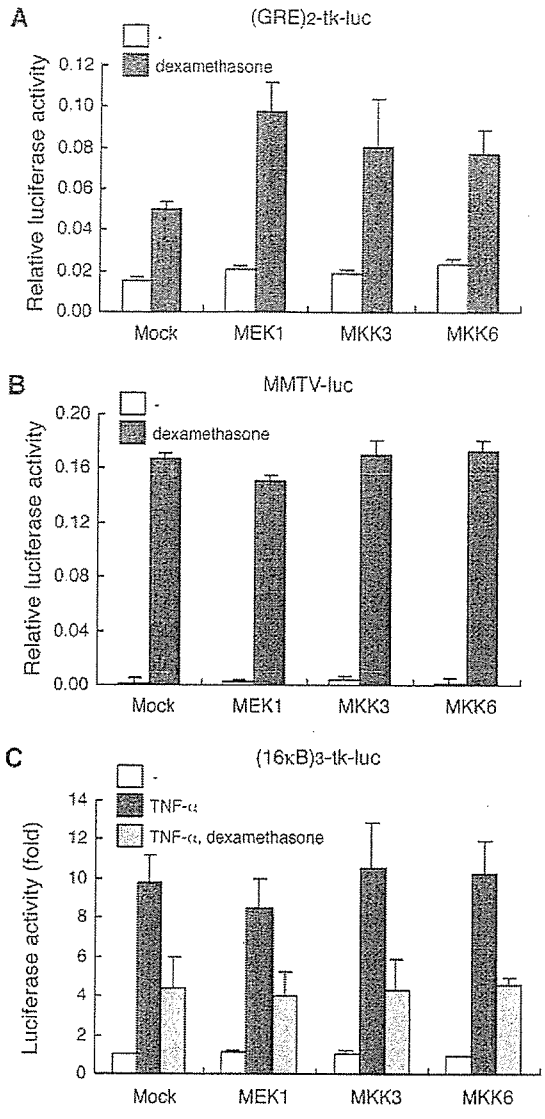

Figure 5. The effect of the activation of ERK or p38 on the transactivation or transrepression function of GR. CC7 cells were transfected with 800 ng GR-dependent luciferase reporter ($(GRE)_2$-tk-luc (**A**) or MMTV-luc (**B**)), 200 ng pRL-CMV, 400 ng pCMX-GR, and 600 ng pcDNA3.1 or an expression vector encoding constitutive-active MEK1, MKK3, or MKK6, and then treated with or without 10^{-6} M dexamethasone for 18 hours. The luciferase activity was measured using the Dual-Luciferase Reporter Assay System (Promega) and normalized by the *Renilla* luciferase activity. (**C**) CC7 cells were transfected with 800 ng NF-κB-dependent luciferase reporter $(16\kappa B)_3$-tk-luc, 200 ng pRL-CMV, 400 ng pCMX-GR, and 600 ng pcDNA3.1 or an expression vector encoding constitutive-active MEK1, MKK3, or MKK6, and then treated with TNF-α in the presence or absence of 10^{-6} M dexamethasone for 24 hours. The luciferase activity in mock-transfected cells with no treatment was set as 1.0.

pro-apoptotic members, such as Bak, Bax, and Bad. Therefore, the steady-state protein expression levels of *bcl*-2, *bcl*-xL, Bak, Bax, and Bad was examined by Western blotting analysis in untreated CC7 cells or CC7 cells treated with U0126 and/or dexamethasone for 24 hours. To lessen the effect of the decrease in the protein level accompanying apoptosis itself, the incubation was performed for 24 hours. The glucocorticoid-induced apoptosis in CCRF-CEM cells is known to become evident after 24 hours [18]. As a result, no remarkable changes in the protein levels were detected. In addition, as other regulators of apoptosis, two IAP family members, c-IAP1 and XIAP, were also analyzed for their protein expression levels; no remarkable changes in the levels of these proteins were detected (Fig. 6).

Effect of U0126 on several dexamethasone-resistant cell lines

As described before, apoptosis was induced in dexamethasone-resistant CC3 cells in the presence of U0126 (Fig. 2B). To examine whether apoptosis is induced in other dexamethasone-resistant cell lines, six human T cell lines, namely Jurkat, JM, RPMI-8402, PEER, CCRF-HSB-2, and HPB-ALL, were tested for annexin V binding in a similar manner. No differences in annexin V binding were found between the presence and absence of 10^{-6} M dexamethasone for each cell line. In the presence of U0126, however, 18.9% ± 4.0% and 28.4% ± 1.3% of PEER and CCRF-HSB-2 cells respectively were positive for annexin V binding in cells, although slight increases in the annexin V binding were detected by treatment with U0126

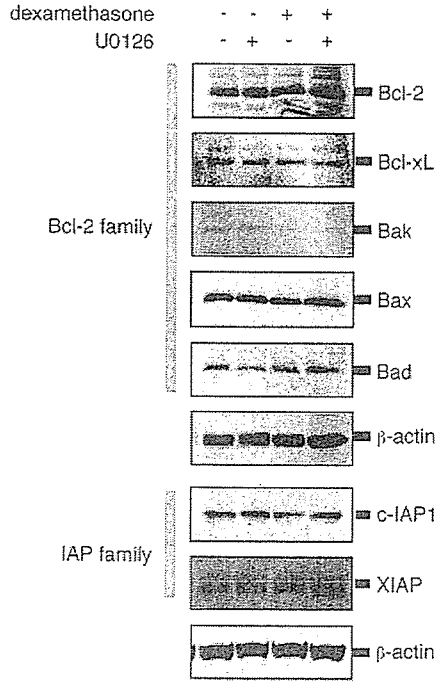

Figure 6. Analysis of the steady-state protein expression levels of *bcl*-2 and IAP family members. CC7 cells were treated with or without 10 μM U0126 in the presence or absence of 10^{-6} M dexamethasone for 24 hours and then lysed with RIPA buffer. A total of 20 μg protein was loaded in each lane. The protein expression levels of *bcl*-2, *bcl*-xL, Bak, Bax, Bad, c-IAP1, XIAP, and β-actin were analyzed with immunoblotting.

alone. No increases in annexin V binding were found in the other four T cell lines by the concomitant use of dexamethasone and U0126 (Fig. 7A). It was investigated whether the treatment of U0126 actually inhibited the activation of ERK in PEER and CCRF-HSB-2 cells, respectively. Phosphorylated ERK1 (p44) and ERK2 (p42) decreased after the treatment of 10 μM U0126 in the absence or the presence of dexamethasone in both cells (Fig. 7B), showing that U0126 inhibits ERK activation in both PEER and CCRF-HSB-2 cells. These results suggest that some of the glucocorticoid-resistant cell lines were converted into glucocorticoid-sensitive cell lines by the inhibition of ERK activation.

Discussion

In this report, the results suggest that ERK inhibits and p38 enhances glucocorticoid-induced T-cell apoptosis at several steps of apoptosis, namely the loss of mitochondrial membrane potential, caspase activation, externalization of phosphatidylserine, DNA fragmentation, and chromatin condensation. This notion was further supported by experiments on the activation of ERK or p38 by transient transfection of constitutive-active MAPKKs or on the inhibition of ERK or p38 by siRNA. Since ERK and p38 are thought to play pivotal roles in differentiation, proliferation, cell survival, and apoptosis in T cell [11,19,20], clarification of the cross-talk with glucocorticoid is extremely intriguing. It may also provide some clues for clarifying the mechanism of glucocorticoid-induced T-cell apoptosis. However, since the roles of both glucocorticoid and MAPKs in apoptosis depend on the cell type, these findings cannot be generalized for all cell types.

Our findings also suggest that ERK and p38 possibly affect the apoptosis process at the premitochondrial or mitochondrial stage (Fig. 8). Among the premitochondrial stages, transcriptional regulation by GR is a possible target of ERK and p38. It was reported that GR was not a direct target of ERK and p38 [21], and that coactivators of GR could be possible targets [22–25]. In our study, both ERK and p38 activated GR-mediated transactivation when $(GRE)_2$-tk-luc was used as the reporter gene, but not when MMTV-luc was used as reporter gene. The effects of ERK and p38 on GR-mediated transactivation might depend on the target genes [26]. On the other hand, neither ERK nor p38 had much effect on the transrepression by GR. In any case, the opposite effects of ERK and p38 on glucocorticoid-induced T-cell apoptosis could not be explained at the level of transcription, although the possibility was not ruled out.

Pro-apoptotic and anti-apoptotic *bcl*-2 family members that regulate apoptosis through mitochondria are other possible targets of ERK and p38. Since the protein levels of several *bcl*-2 members were not changed after treatment with U0126, we could not identify the targets of ERK. One possibility is that the phosphorylation status or subcellular localization of *bcl*-2 family members might be changed by ERK [27,28].

It is known that glucocorticoid induces G1 arrest in the cell cycle in glucocorticoid-induced T-cell apoptosis [29]. It was reported that p38 was necessary for G1 arrest in cycling cells [12]. It was hypothesized that p38 was necessary

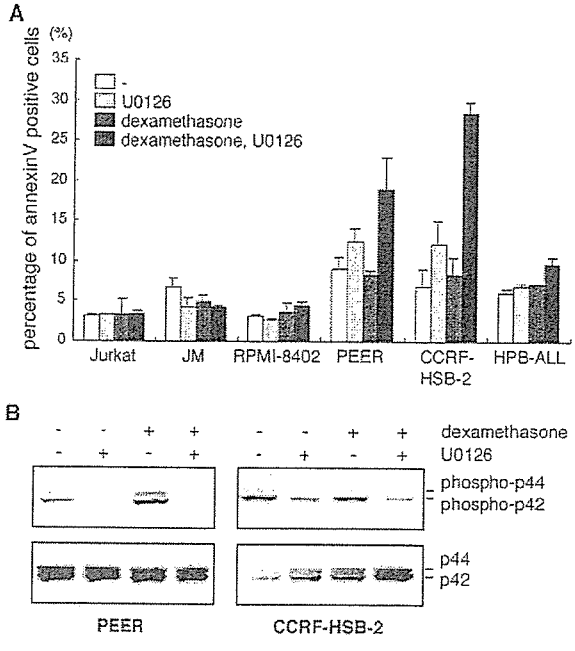

Figure 7. Effects of U0126 on glucocorticoid-induced apoptosis in several dexamethasone-resistant cell lines. (A) Six human T cell lines, namely Jurkat, JM, RPMI-8402, PEER, CCRF-HSB-2, and HPB-ALL, were treated with or without 10 μM U0126 in the presence or absence of 10^{-7} M dexamethasone for 48 hours, and then analyzed for annexin V binding. (B) PEER and CCRF-HSB-2 cells were treated with or without 10^{-6} M dexamethasone in the presence or absence of 10 μM U0126 for 24 hours. Cell lysate was subjected to immunoblotting with anti-phospho ERK1/2 antibody or anti-ERK1/2 antibody.

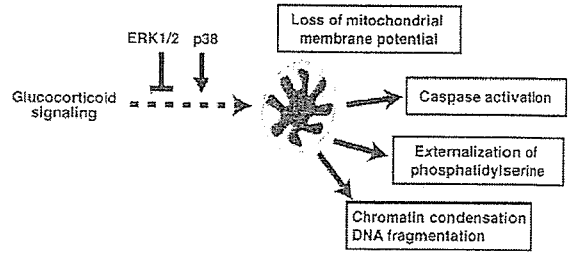

Figure 8. ERK1/2 and p38 possibly affect the apoptotic process at the premitochondrial or mitochondrial stage. After the apoptotic signal reaches the mitochondria, several factors are released from the intermembrane space, leading to activation of the apoptosis cascade. Apoptosis through mitochondria is regulated by *bcl*-2 family members. See the text for details. ERK and p38 are supposed to affect the apoptosis process at the premitochondrial or mitochondrial stage.

for G1 arrest in glucocorticoid-induced T-cell apoptosis, but SB203580 alone had little effect on the cell cycle itself in CC7 cells (Fig. 3C and data not shown). Thus, this hypothesis seems to be unlikely.

ERK is mainly activated by the Ras-Raf pathway [9]. The Ras-Raf-ERK pathway is activated through the stimulation of T-cell receptor or by several growth factors. The finding that ERK inhibits glucocorticoid-induced T-cell apoptosis, although reported by others [26,30,31], explains the fact that apoptosis through T-cell receptor antagonizes glucocorticoid-induced apoptosis . Moreover, it was shown in this report that inhibition of the ERK pathway restored dexamethasone sensitivity in some glucocorticoid-resistant T cells. This is especially significant when considering clinical measures for glucocorticoid resistance. The combination of both inhibitors of the ERK activation pathway and glucocorticoid may help us to cope with glucocorticoid resistance. Regarding the reason why inhibition of ERK did not restore dexamethasone sensitivity in all the glucocorticoid-resistant T cell lines, there are several possibilities. One is that some of the cells may be devoid of functional GR. Another is that the survival of some cells may depend principally on other signals including that of PI3-kinase.

A variety of signals including lipopolysaccharide (LPS), inflammatory cytokines such as TNF-α and IL-1, hormones, G protein–coupled receptors, osmotic and heat shock, and other stresses activate p38 [12]. Some of these stimuli may also be used with glucocorticoid to overcome glucocorticoid resistance.

Experimental procedures

Reagents

Dexamethasone, antibody for β-actin and HRP-conjugated anti-goat IgG were purchased from Sigma (St. Louis, MO, USA), U0126 and SB203580 were from Calbiochem (San Diego, CA, USA), TNF-α was from R&D Systems, Inc. (Minneapolis, MN, USA), and JC-1, $DiOC_6(3)$ and Hoechst 33342 were from Molecular Probes, Inc. (Eugene, OR, USA). The antibodies for ERK1/2, p38 MAPK, JNK/SAPK, phospho-ERK1/2, phospho-p38 MAPK, phospho-JNK/SAPK, Bax, HRP-conjugated anti-mouse IgG, and HRP-conjugated anti-rabbit IgG were from Cell Signaling Technology, Inc. (Beverly, MA, USA). Antibodies for *bcl*-2, *bcl*-xL, Bak, Bad, c-IAP1, and XIAP were from Santa Cruz Biotechnology, Inc. (Santa Cruz, CA, USA). pRL-CMV was from Promega Co. (Madison, WI, USA). pEGFP-C1 was from Clontech (Palo Alto, CA, USA). pcDNA3.1 was from Invitrogen Co. (Carlsbad, CA, USA). pFR-luc, pFC-MEK1, pFC-MKK3, pFC-MEKK, pFA2-Elk1, pFA2-CHOP, and pFA2-cJun were from Stratagene (La Jolla, CA, USA). siRNAs for ERK1, ERK2, p38α, p38β, and FAM-labeled control siRNA were obtained from Ambion (Austin, TX, USA).

Plasmid construction

pcDNA3.1-MKK6-SETE was a kind gift from Dr. Yukiko Gotoh (Tokyo, Japan). Human MEK5 cDNA was amplified by RT-PCR method with ExTaq (Takara, Japan) and cloned into pTarget mammalian expression vector (Promega, Madison, WI, USA). The primers used for the amplification were 5′-ATGCTGTGGCTAGCCCTTGGC-3′ and 5′-TCACGGGGGCCCCTGCTGG-3′. Constitutive active form of MEK5, MEK5-SDTD [32], was constructed by replacing both Ser313 and Thr317 with Asp with Site-directed II mutagenesis kit (Stratagene, La Jolla, CA, USA). The mutagenesis primers were 5′-GCACTCAGCTGGTGAATGATATAGCCAAGGATTATGTTGGAACAAATGC-3′ and 5′-GCATTTGTTCCAACATAATCCTTGGCTATATCATTCACCAGCTGAGTGC-3′. cDNA sequence of MEK5-SDTD was confirmed with sequence analysis. The firefly-luciferase reporter vector and MMTV-luc have been described previously [33]. tk-Luc was constructed by cloning the −109 to +37 region of the herpesvirus thymidine kinase promoter into the *Bgl* II and *Hind* III sites of the pGL3-basic vector (Promega, Madison, WI, USA). A pair of oligonucleotides, 5′-TAGCCCCTTGGAAATTCCGGAGCTTGGAAATTCCGGAGCTTGGA AAT TCCGGAG-3′ and 5′-TCGACTCCGGAATTTCCAAGCTCCGGAATTTCCAAG CTCCGGAATTTCCAAGGGGCTA-3′, were annealed, resulting in a double-stranded oligonucleotide with both a blunt end and a *Xho* I–compatible overhang that was then inserted into the *Sma* I and *Xho* I sites of tk-Luc, giving rise to $(16\kappa B)_3$-tk-Luc containing three copies of the κB sites found in the human ICAM-1 gene promoter [34]. A pair of oligonucleotides, 5′-GTTACAAACTGTTCTGTTACAAACTGTTCT-3′ and 5′-TCGAAGA ACAGTTTGTAACAGAACAGTTTGTAAC-3′, were annealed, resulting in a double-stranded oligonucleotide with both a blunt end and a *Xho* I–compatible overhang that was then inserted into the *Sma* I and *Xho* I sites of tk-Luc, giving rise to $(GRE)_2$-tk-Luc containing two copies of the glucocorticoid response element (GRE) [35].

Cell culture and limiting dilution

All the human T cell lines, except for CCRF-CEM, were provided by the Fujisaki Cell Center (Hayashibara Biochemical Laboratories, Inc., Okayama, Japan). CCRF-CEM was obtained from Dainippon Pharmaceutical Co. Ltd. (Osaka, Japan). Fetal bovine serum was treated with dextran-coated charcoal as described previously [36]. Cells were cultured in RPMI 1640 supplemented with 10% fetal bovine serum (FBS), 100 U/mL penicillin, 100 μg/mL streptomycin, 292 μg/mL L-glutamine, and 5 μM 2-mercaptoethanol. Regarding the limiting dilution, CCRF-CEM cells were diluted in a volume of 300 μL at a density of 1 cell/mL in 96-well plates. The wells containing a single cell, as observed under a microscope, were selected for isolating subclones.

Detection of apoptosis

Externalization of phosphatidylserine was detected with an annexin V–FITC kit (Immunotech Co., Marseilles, France) or annexin V–PE (Pharmingen, San Diego, CA, USA). Briefly, cells were washed with phosphate-buffered saline (PBS) and resuspended with annexin V binding buffer, followed by the addition of annexin V and PI. The cells were analyzed using an EPICS flow cytometer (Beckman Coulter, Inc., Miami, FL, USA) or a FACScan (BD Biosciences, San Diego, CA, USA), and the percentage of annexin V–binding cells was calculated. Regarding the loss of mitochondrial membrane potential, 2×10^5 CC7 cells were incubated in culture medium containing 5 μM JC-1 or 40 μM $DiOC_6(3)$ at 37°C for 30 minutes, and then analyzed using a FACScan. Activated caspase-3 was detected with PE-conjugated anti-active caspase-3 antibody (Pharmingen). Anti-active caspase-3 antibody recognizes the heterodimer of 17- and 12-kDa subunits that were derived from the 32-kDa proenzyme. Approximately 1×10^6 cells were fixed in PBS containing 1% paraformaldehyde, permeabilized, and stained intracellularly in PBS containing 0.1% saponin and 4% FBS. Cells were then washed twice in PBS containing 4% FBS and analyzed on a FACScan flow cytometer. Regarding the degradation of DNA, 1×10^6 CC7 cells were washed with ice-cold PBS, resuspended with 2 mL of ice-cold 70% ethanol, and then incubated for 4 hours at 4°C. The cells were washed with PBS twice, resuspended with 1 mL of PBS containing 10 μg/mL RNase A, incubated for 30 minutes at 37°C, and propidium iodide was added to a final concentration of 10 μg/mL. The PI intensity was measured for 1×10^5 events using a FACScan, and the percentage of the sub-G_0/G_1 fraction was analyzed using CellQuest software. To assess the apoptotic nuclear morphology, CC7 cells were stained with 2 ng/mL Hoechst 33342, and observed under a confocal microscope (Leica Microsystems, Wetzlar, Germany).

Transfection

CC7 cells were transfected using Nucleofector (Amaxa Biosystems, Cologne, Germany) according to the manufacturer's instruction. Briefly, 5×10^6 CC7 cells were washed with PBS, resuspended with the cell line nucleofector kit V solution, and mixed with plasmid DNA in a total volume of 100 μL. The cell mixture was transferred to a cuvette and transfected with program C-16 using Nucleofector. Transfected cells were cultured in 2 mL RPMI 1640 medium at 37°C for 3 hours, and treated with various stimuli.

Real-time PCR

After total RNA was purified with RNeasy kit (Qiagen, Tokyo, Japan), first-strand cDNA synthesis was performed with QuantiTect reverse transcription kit (Qiagen). Primers were designed using Primer Express software (Applied Biosystems, Foster City, CA, USA). The primers used were follows: 5′-CCTTCCAACCTGCTGCTCAAC-3′ and 5′-TTCTGTCAGGAACCCTGTGTGATC-3′ for ERK1, 5′-ACCTGCTGGA CCGGATGTTAA-3′ and 5′-GGTGAGC-CAGCGCTTCCT-3′ for ERK2, 5′-TGTGAATGAA-GACTGTGAGCTGAAGATT-3′ and 5′-GCCACGTAGC CTGTCATTTCATC-3′ for p38α, and 5′-CTTGGAAG-GATGCTGGTGCT-3′ and 5′-CCTCAACGCTCTCATCA-TATGG-3′ for p38β. Samples were subjected to real-time PCR with SYBR Premix Ex Taq (TAKARA) using LightCycler (Roche, Mannheim, Germany). Using comparative delta Ct method, the mRNA level of target gene was calculated.

Luciferase assay

Luciferase assays were performed using the Dual-Luciferase Reporter Assay System (Promega, Madison, WI, USA) according to the manufacturer's instructions. Two $\times 10^5$ CC7 cells were washed with PBS and lysed with 100 μL of passive lysis buffer. Fifty μL of the lysate was subjected to the luciferase assay. The luciferase activity was detected with a Lumat LB 9507 luminometer (Berthold Technology Co., Bad Wildbad, Germany).

Immunoblotting

Cells were washed with PBS and lysed with RIPA buffer (1% Nonidet P-40, 0.5% sodium deoxycholate, 0.1% sodium dodecyl sulfate [SDS], Complete Mini Protease Inhibitor Cocktail [Roche Diagnostics, Mannheim, Germany] in PBS). The lysates were collected and centrifuged at 15,000 rpm for 15 minutes at 4°C. The protein concentrations were measured with BCA protein assay (Pierce, Rockford, IL, USA). A total of 20 μg protein was subjected to SDS-PAGE and transferred onto a PVDF membrane (Bio-Rad Laboratories, Hercules, CA, USA). The membrane was incubated in blocking buffer (5% nonfat skim milk in PBS or Tris-buffered saline (TBS) containing 0.05% Tween-20) for 1 hour. The membrane was incubated for 2 hours in the primary antibody, washed with PBS or TBS containing 0.05% Tween-20, and then incubated for 1 hour in the secondary antibody. The protein expression levels were visualized with an ECL Plus kit (Amersham Biosciences, Buckinghamshire, England) and a STORM8600 image analyzer (Amersham Biosciences).

References

1. Distelhorst CW. Recent insights into the mechanism of glucocorticosteroid-induced apoptosis. Cell Death Differ. 2002;9:6–19.
2. Montague JW, Cidlowski JA. Glucocorticoid-induced death of immune cells: mechanisms of action. Curr Top Microbiol Immunol. 1995;200: 51–65.
3. Cidlowski JA, King KL, Evans-Storms RB, Montague JW, Bortner CD, Hughes FM Jr. The biochemistry and molecular biology of glucocorticoid-induced apoptosis in the immune system. Recent Prog Horm Res. 1996:51:457–490.
4. Thompson EB. Apoptosis and steroid hormones. Mol Endocrinol. 1994;8:665–673.
5. Gross A, McDonnell JM, Korsmeyer SJ. BCL-2 family members and the mitochondria in apoptosis. Genes Dev. 1999:13:1899–1911.

6. Adams JM, Cory S. The Bcl-2 protein family: arbiters of cell survival. Science. 1998;281:1322–1326.
7. Wang X. The expanding role of mitochondria in apoptosis. Genes Dev. 2001;15:2922–2933.
8. Hengartner MO. The biochemistry of apoptosis. Nature. 2000;407: 770–776.
9. Pearson G, Robinson F, Beers Gibson T, et al. Mitogen-activated protein (MAP) kinase pathways: regulation and physiological functions. Endocr Rev. 2001;22:153–183.
10. Hayashi M, Lee JD. Role of the BMK1/ERK5 signaling pathway: lessons from knockout mice. J Mol Med. 2004;82:800–808.
11. Dong C, Davis RJ, Flavell RA. MAP kinases in the immune response. Annu Rev Immunol. 2002;20:55–72.
12. Kyriakis JM, Avruch J. Mammalian mitogen-activated protein kinase signal transduction pathways activated by stress and inflammation. Physiol Rev. 2001;81:807–869.
13. Widmann C, Gibson S, Jarpe MB, Johnson GL. Mitogen-activated protein kinase: conservation of a three-kinase module from yeast to human. Physiol Rev. 1999;79:143–180.
14. Johnson GL, Lapadat R, Sugita M, et al. Mitogen-activated protein kinase pathways mediated by ERK, JNK, and p38 protein kinases. Science. 2002;298:1911–1912.
15. Norman MR, Thompson EB. Characterization of a glucocorticoid-sensitive human lymphoid cell line. Cancer Res. 1977;37:3785–3791.
16. Yuh YS, Thompson EB. Complementation between glucocorticoid receptor and lymphocytolysis in somatic cell hybrids of two glucocorticoid-resistant human leukemic clonal cell lines. Somat Cell Mol Genet. 1987;13:33–45.
17. Kroemer G, Reed JC. Mitochondrial control of cell death. Nat Med. 2000;6:513–519.
18. Thompson EB, Medh RD, Zhou F, et al. Glucocorticoids, oxysterols, and cAMP with glucocorticoids each cause apoptosis of CEM cells and suppress c-myc. J Steroid Biochem Mol Biol. 1999;69: 453–461.
19. Tanaka N, Kamanaka M, Enslen H, et al. Differential involvement of p38 mitogen-activated protein kinase kinases MKK3 and MKK6 in T-cell apoptosis. EMBO Rep. 2002;3:785–791.
20. Werlen G, Hausmann B, Naeher D, Palmer E. Signaling life and death in the thymus: timing is everything. Science. 2003;299:1859–1863.
21. Rogatsky I, Logan SK, Garabedian MJ. Antagonism of glucocorticoid receptor transcriptional activation by the c-Jun N-terminal kinase. Proc Natl Acad Sci U S A. 1998;95:2050–2055.
22. Knutti D, Kressler D, Kralli A. Regulation of the transcriptional coactivator PGC-1 via MAPK-sensitive interaction with a repressor. Proc Natl Acad Sci U S A. 2001;98:9713–9718.
23. Rowan BG, Garrison N, Weigel NL, O'Malley BW. 8-Bromo-cyclic AMP induces phosphorylation of two sites in SRC-1 that facilitate ligand-independent activation of the chicken progesterone receptor and are critical for functional cooperation between SRC-1 and CREB binding protein. Mol Cell Biol. 2000;20:8720–8730.
24. Font de Mora J, Brown M. AIB1 is a conduit for kinase-mediated growth factor signaling to the estrogen receptor. Mol Cell Biol. 2000;20:5041–5047.
25. Liu YZ, Chrivia JC, Latchman DS. Nerve growth factor up-regulates the transcriptional activity of CBP through activation of the p42/p44(MAPK) cascade. J Biol Chem. 1998;273:32400–32407.
26. Jamieson CA, Yamamoto KR. Crosstalk pathway for inhibition of glucocorticoid-induced apoptosis by T cell receptor signaling. Proc Natl Acad Sci U S A. 2000;97:7319–7324.
27. Huang ST, Cidlowski JA. Phosphorylation status modulates Bcl-2 function during glucocorticoid-induced apoptosis in T lymphocytes. FASEB J. 2002;16:825–832.
28. Hsu YT, Wolter KG, Youle RJ. Cytosol-to-membrane redistribution of Bax and Bcl-X(L) during apoptosis. Proc Natl Acad Sci U S A. 1997; 94:3668–3672.
29. King KL, Cidlowski JA. Cell cycle regulation and apoptosis. Annu Rev Physiol. 1998;60:601–617.
30. Tsitoura DC, Rothman PB. Enhancement of MEK/ERK signaling promotes glucocorticoid resistance in $CD4^+$ T cells. J Clin Invest. 2004; 113:619–627.
31. Spinetti G, Bernardini G, Camarda G, et al. The chemokine receptor CCR8 mediates rescue from dexamethasone-induced apoptosis via an ERK-dependent pathway. J Leukoc Biol. 2003;73:201–207.
32. Kato Y, Kravchenko VV, Tapping RI, Han J, Ulevitch RJ, Lee JD. BMK1/ERK5 regulates serum-induced early gene expression through transcription factor MEF2C. EMBO J. 1997;16:7054–7066.
33. Adachi M, Takayanagi R, Tomura A, et al. Androgen-insensitivity syndrome as a possible coactivator disease. N Engl J Med. 2000;343: 856–862.
34. van de Stolpe A, Caldenhoven E, Stade BG, et al. 12-O-tetradecanoylphorbol-13-acetate- and tumor necrosis factor α-mediated induction of intercellular adhesion molecule-1 is inhibited by dexamethasone. Functional analysis of the human intercellular adhesion molecular-1 promoter. J Biol Chem. 1994;269:6185–6192.
35. Evans RM. The steroid and thyroid hormone receptor superfamily. Science. 1988;240:889–895.
36. Okabe T, Haji M, Takayanagi R, et al. Up-regulation of high-affinity dehydroepiandrosterone binding activity by dehydroepiandrosterone in activated human T lymphocytes. J Clin Endocrinol Metab. 1995;80: 2993–2996.

話　題

アンドロゲン受容体欠損マウスと肥満*

柳　瀬　敏　彦**

Key Words : testosterone, estrogen, androgen receptor, obesity, metabolic syndrome

はじめに

近年，内臓脂肪型肥満，高中性脂肪血症，低HDL血症，高血圧，耐糖能異常を主病態とするメタボリックシンドローム(MS)が，LDL-コレステロールとは独立した動脈硬化性疾患の診療ターゲットとして注目されている．性ステロイドはMSの性差を説明する重要な背景因子であるが，研究成績は比較的少ない．一般に男性では中高年以降，上半身型の脂肪蓄積パターンを示すようになり，MSの発症リスクの増大と関連する．この背景には，加齢に伴うテストステロン(T)の低下変動がその一因として関与する可能性が考えられる．最近，Tの作用不全モデルであるアンドロゲン受容体ノックアウト(ARKO)マウスではオス特異的に晩発性に肥満を呈することが明らかとなった[1]．われわれは内因性TのMSにおける意義を明らかにする目的でARKOマウスの肥満機序に関する解析を行ったので，紹介する．

テストステロンと内臓脂肪肥満

近年，Tが，男性における体構成を決める重要な因子であるとする成績が蓄積されつつある．男性において脂肪蓄積の程度は血中T値と逆相関するとの成績を認める[2]．われわれは腹部臍高のCT断面のV/S比の評価による男性の内臓脂肪の割合も加齢とともに増加することを認めた(図1)．一方，性腺機能低下症の男性では，加齢

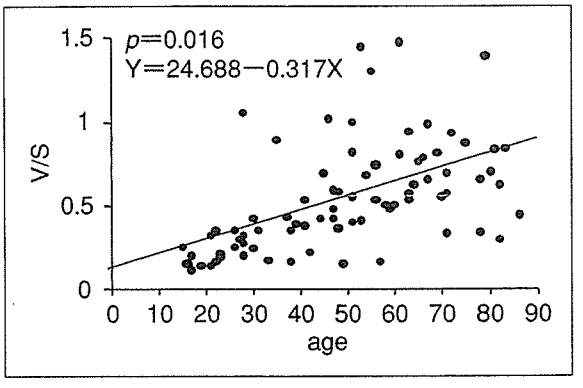

図1　男性における内臓脂肪/皮下脂肪(V/S)と加齢(自験成績)

とともに体脂肪の有意の増加を認め，それはTの投与によって減少することが報告されている[3]．さらに，若年健康成人の内因性血中Tレベルをゴナドトロピン放出ホルモンアナログの投与によって低下させた場合には，体脂肪率の増加と安静時エネルギー消費量の低下が認められている(図2)[4]．これらの事実は，内因性のテストステロンはヒトにおいて，エネルギー消費を高め，体脂肪を減らす方向に作用している可能性を示唆する．実際，*in vitro*では，アンドロゲンは脂肪分解を促進する方向に作用していることが，示されている．また，ゴナドトロピン放出ホルモンアンタゴニストの投与によって内因性のTを低下させて際には，脂肪組織由来のインスリン抵抗性改善作用物質として最近，注目されている血中adiponectin濃度が上昇し，同時に外因

* Androgen receptor knockout mouse and obesity.

** Toshihiko YANASE, M.D.: 九州大学大学院医学研究院病態制御内科〔〒812-8582 福岡市東区馬出3-1-1〕; Department of Medicine and Bioregulatory Science, Graduate School of Medical Sciences, Kyushu University, Fukuoka 812-8582, JAPAN

性のTの補充をした場合には，その上昇が抑制されること，また外因性にTを単独で投与した際にも血中adiponectin濃度が低下することが報告されている[5]．

内因性のTの体脂肪減少効果の詳細な機序は明らかではなかった．このことを以下のアンドロゲン受容体ノックアウトマウスを用いて解析した．

アンドロゲン受容体ノックアウトマウスの肥満機序

アンドロゲン受容体遺伝子はX染色体上に存在し，ヒトではその異常は睾丸性女性化症をひき起こす．本邦のKato S[1]のグループならびに米国のChang[6]のグループがそれぞれ独立にアンドロゲン受容体(AR)ノックアウトマウス(ARKOマウス)の作製に成功した．このマウスでは睾丸性女性化症の表現型が再現されると同時に骨粗鬆症や肥満がひき起こされることが明らかにされた．ただし，このマウスでは著しい睾丸萎縮のために血中T値は低下する点が，同レベルが正常か，軽度上昇を示すヒトの睾丸性女性化症の病態と若干，異なる点である．ARKOのオスマウスでは晩発性に，皮下，および腹部内臓周囲の白色脂肪組織(WAT)の増加と肥満をきたすことが明らかになった(図3)[7]．ヒトにおけるARの遺伝的異常でひき起こされる睾丸性女性化症では，血中T値は正常もしくは高値となるが，本マウスでは，高度の精巣委縮のためにT値は低下していた．基質であるTの低下のためにアロマターゼ活性を介したエストロゲンの産生が低い可能性が考えられるが，実際には本マウスの血中E_2濃度は正常であり，肥満は少なくとも低エストロゲン血症によってひき起こされたものではないと考えられた．

40週齢のARKOオスマウスでは皮下および腹部内臓周囲のWATの増加と肥満をきたしたが，CT評価にてとくに内臓脂肪の増加が顕著であった(図3A～C)．このような現象はメスのARKOマウスでは観察されず，オスに特有の現象と考えられた．ARKOオスマウスでは野性型に比して，食餌摂取量や血中蛋白，脂質濃度には差を認めなかったが，自発運動量(図3D)と酸素消費量

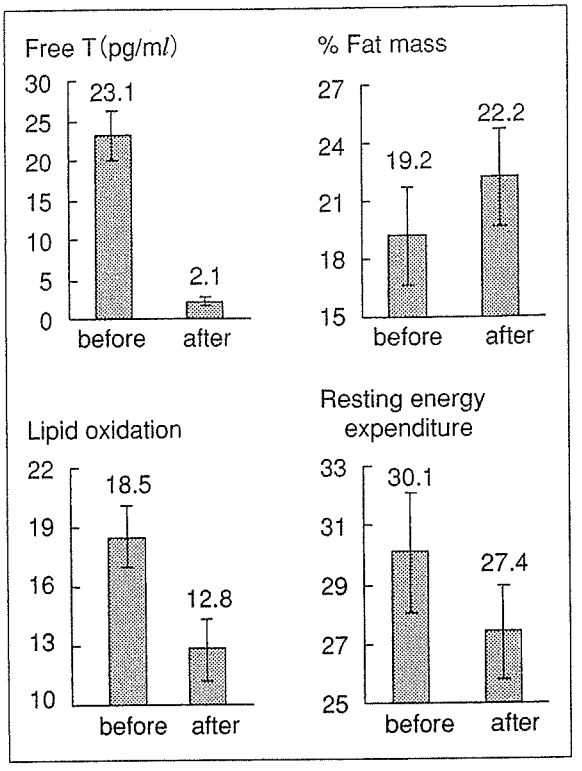

図2　健康若年男子においてGnRH製剤10週投与により性腺機能低下をひき起こした際の各種指標の変化　(文献[10]より引用改変)

(図3E)の有意の低下を認め，肥満の機序としてエネルギー消費の低下が原因と考えられた．興味深いことにARはWATで褐色脂肪組織の約7倍の発現を認め，その意義はWATで大きいと考えられた．そのことを反映するように，ARKOマウスの褐色脂肪組織における熱産生蛋白のUCP-1の発現低下は野性型の約50%にとどまったが，WATでは，約7%と顕著な発現低下を認めた(図4A)．また，ARKOマウスの白色脂肪組織では，脂肪分解系酵素のホルモン感受性リパーゼ(HSL)の顕著な発現低下を認めたが(図4B)，脂肪合成系各種酵素，蛋白の発現は野性型と同等で，WAT増加の原因として脂肪分解の低下が一因と考えられた．また，血中インスリン基礎値はARKOオスマウスで野生型オスマウスに較べ高値傾向を認めたが有意ではなかった．高インスリン負荷試験ならびに糖負荷試験における血糖，血中インスリンの反応性は，野性型とARKOマウスで差異を認めず，肥満にもかかわらず，個体全体としての耐糖能とインスリン感受性はほぼ正常と考えられた(図4C)．興味深いことに，ARKOマウスにおける血中のadiponectin濃度は有意に増

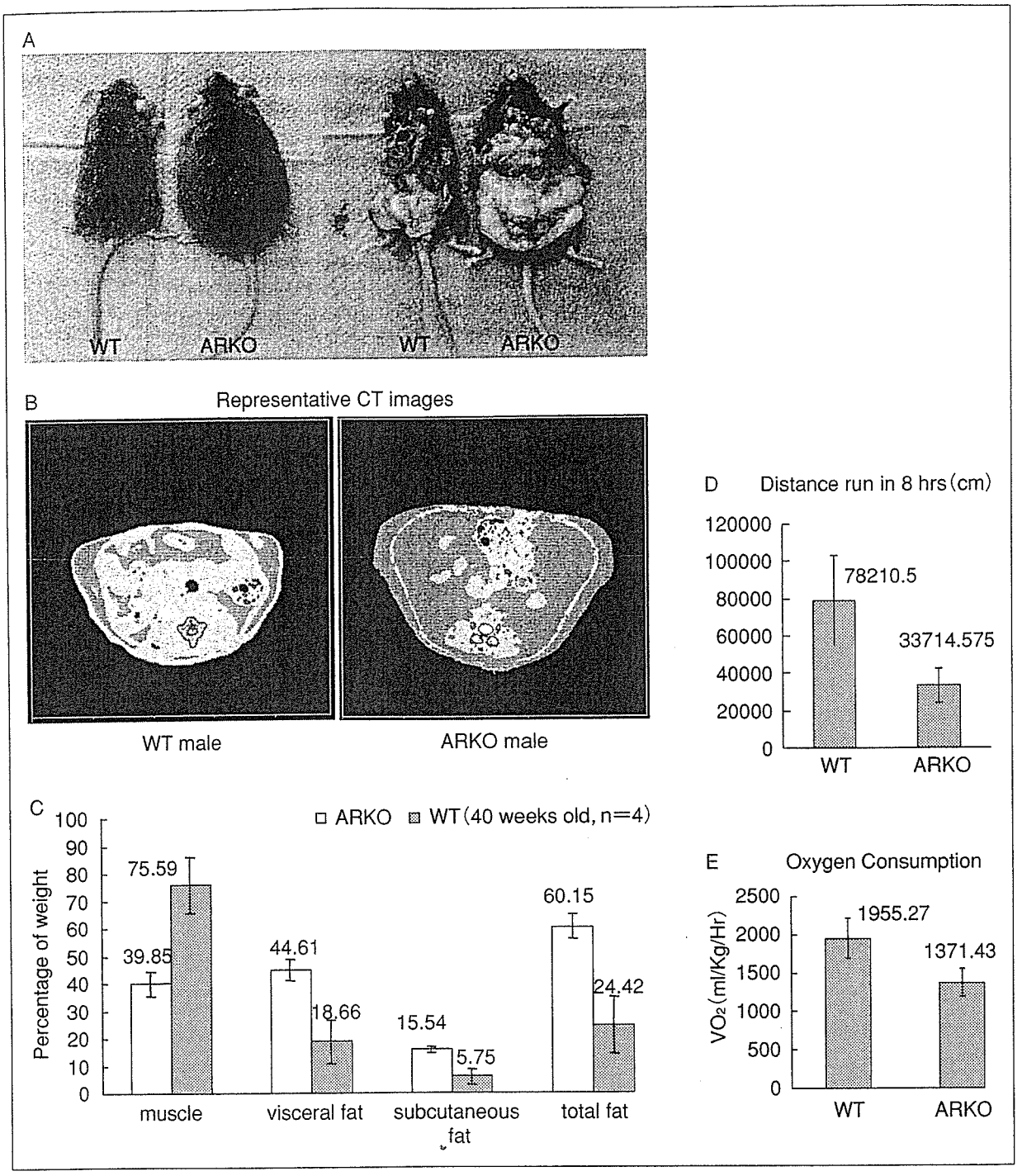

図3　アンドロゲン受容体ノックアウト(ARKO)マウスの肥満所見(A, B)とエネルギー代謝(C, D, E)
A：オス野性型マウスとオスARKOマウスの肉眼所見(40週齢)．B：L3レベルのCT写真(40週齢)．赤が内臓脂肪，黄色が皮下脂肪．C：CT解析に基づく体構成(n=4)．D：40週齢マウスにおける自発運動量(8時間における走行距離)(各群n=6)．E：40週齢マウスにおける酸素消費量(各群n=6)　(文献[7]より引用)

加していた(図4D)．

以上より，ARKOマウスの肥満の成因にはエネルギー消費の低下と脂肪分解系酵素の低下が関与すると考えられた．一方，肥満を呈しながら本マウスの耐糖能ならびにインスリン感受性は正常であったが，その原因としてインスリン感受性促進効果をもつ血中adiponectin濃度の高値が一因と考えられた．Nishizawaら[8]は，Tは脂肪細胞よりのadiponectin分泌を抑制することを報告しており，本マウスの血中adiponectin濃度の上昇を説明するものと考えられる．これらのデータはヒト男性における既述のTのadiponectin分

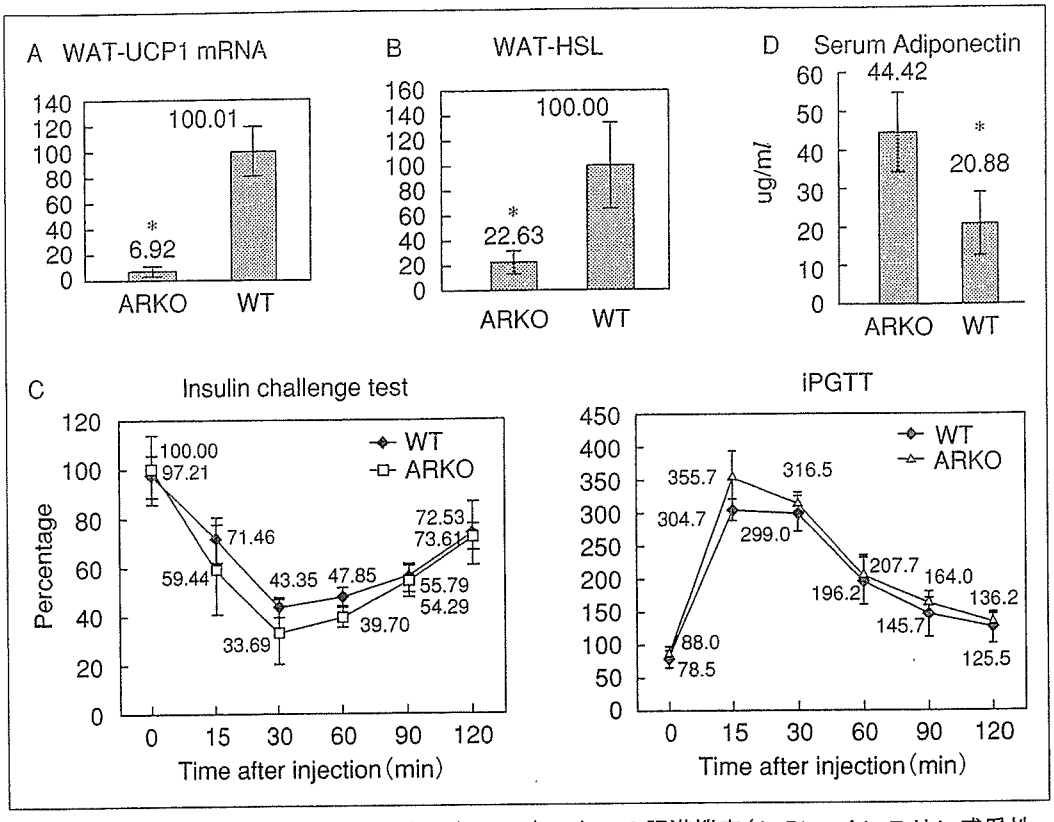

図4　アンドロゲン受容体ノックアウト(ARKO)マウスの肥満機序(A, B)，インスリン感受性(C, D)および耐糖能(E)

A：白色脂肪組織(WAT)におけるUCP-1の発現(各群 n＝6)．B：WATにおけるhormone sensitive lipase(HSL-1)の発現(各群 n＝6)．C：インスリン負荷試験(左)と糖負荷試験．D：血中adiponectin濃度(各群 n＝6)．*p＜0.01　(文献[7]より引用)

泌低下作用をよく説明する．内因性テストステロンはインスリン抵抗性に関しては，adiponectinの低下を介して増悪の方向に作用していると考えられる．なお，最近，Changらのグループもわれわれ同様，ARKOオスマウスでは晩発性肥満をきたすことを報告しているが，彼らの検討の範囲ではインスリン抵抗性と耐糖能異常も認めたとしている[9]．マウス成育環境の違いにより肥満のみならず，適応破綻によりすでにインスリン抵抗性の出現に至った状態と考えられる．

一方，エストロゲン欠乏症のaromatase(エストロゲン合成酵素)KOマウスでも肥満とインスリン抵抗性が報告されている[10]．同マウスではWATにおける脂肪合成亢進が認められており[11]，同じ肥満でも，ARKOマウスとは肥満機序が異なる．なお，ARKOマウスでは，血中E_2濃度は正常であり，肥満は少なくとも低エストロゲン血症によってひき起こされたものではない．以上の成績を基に内因性のTとエストロゲンの脂肪代謝に及ぼす作用について，表1に対比させる形でまとめた．Tならびにエストロゲンはともに抗肥満作用をもつと考えられるが，インスリン感受性に関しては，Tは増悪，エストロゲンは改善の方向に作用すると考えられた．

おわりに

ARKOマウスではオス特異的に晩発性の肥満をきたし，その成因として，WATのUCP-1の発現低下に伴うエネルギー消費の低下と脂肪分解の抑制が関与することを明らかにした．高年以降のいわゆる「中年太り」には加齢に伴う基礎代謝の低下が関与するが，オスARKOマウスはその病態モデルとも言え，加齢に伴う男性肥満にはテストステロン濃度の低下や作用不全の関与が示唆される．中高年以降のいわゆる「中年太り」や生活習慣病の発症要因の一因として，加齢に伴うTの低下が関係している可能性が考えられる．内臓脂肪蓄積を抑制するような代謝に特化した

表1 内因性のテストステロンとエストロゲンの脂肪代謝に関する比較

	テストステロン	エストロゲン
脂肪蓄積(肥満)	↓	↓
脂肪合成	～	↓
脂肪分解	↑	～
インスリン抵抗性	↑	↓
adiponectin	↓	～

男性ホルモン作用を有し，前立腺刺激作用を有さぬようなselective androgen receptor modulator(SARM)の開発が可能になれば，今後，中高年以降の生活習慣病治療薬の一つとして有望かもしれない．

文　献

1) Sato T, Matsumoto T, Yamada T, et al. Late onset of obesity in male androgen receptor-deficient(ARKO) mice. Biochem Biophys Res Commun 2003 ; 300 : 167.
2) Kyle UG. Genton L, Hans D, et al. Age-related difference in fat-free mass, skeletal muscle, body cell mass and fat mass between 18 and 94 years. Eur J Clin Nutr 2001 ; 55 : 663.
3) Synder PJ, Peachery H, Berlin JA, et al. Effects of testosterone replacement in hypogonadal men. J Clin Endocrinol Metab 2000 ; 65 : 2670.
4) Mauras N, Hayes V, Welch S, et al. Testosterone deficiency in young men : marked alterations in whole body protein kinetics, strength, and adiposity. J Clin Endocrinol Metab 1998 ; 83 : 1886.
5) Page ST, Herbst KL, Amory JK, et al. Testosterone administration suppresses adiponectin levels in men. J Androl 2005 ; 26 : 85.
6) Yeh S, Tsai MY, Xu Q, et al. Generation and characterization of androgen receptor knockout(ARKO) mice : an *in vivo* model for the study of androgen functions in selective tissues. Proc Natl Acad Sci USA 2002 ; 99, 13498.
7) Fan W, Yanase T, Nomura M, et al. Androgen receptor null malemice develop late-onset obesity due to decreased energy expenditure and lypolytic activity but show normal insulin sensitivity with high adiponectin secretion. Diabetes 2005 ; 54 : 1000.
8) Nishizawa, H. Shimomura I, Kishida K, et al. Androgens decrease plasma adiponectin, an insulin-sensitizing adipocyte-derived protein. Diabetes 2002 ; 51 : 2734.
9) Lin HY, Xu Q, Yeh S, et al. Insulin and Leptin Resistance With Hyperleptinemia in Mice Lacking Androgen Receptor Diabetes 2005 ; 54 : 1717.
10) Jones MEE, Thorburn AW, Britt KL, et al. Aromatase deficient(ArKO) mice have a phenotype of increased adiposity. Proc Natl Acad Sci USA 2000 ; 97 : 12735.
11) Misso ML, Murata Y, Boon WC, et al. Cellular and molecular characterization of the adipose phenotype of the aromatase-deficient mouse. Endocrinol 2003 ; 144 : 1474.

*　　*　　*

特集　アンドロロジー―課題と展望

アンドロゲン測定の現状と問題点*

柳瀬敏彦**

Key Words：total-testosterone, free-testosterone, bioavailable testosterone

はじめに

血中テストステロンの95％以上は精巣ライデイツヒ細胞由来で，残りの５％は主に副腎においてアンドロステンジオンなどの他のステロイドから生成される．下垂体から分泌されたLHは精巣のライデイツヒ細胞の細胞膜に作用してcyclic AMPの上昇を介してテストステロンの合成，分泌を刺激する．一方，テストステロンは，ネガテイブフィードバックによりLH分泌を抑制する．血漿中のテストステロンの約98％はsex hormone-binding globulin(SHBG)やアルブミンと結合している蛋白結合型であり，1～2％が遊離型として存在している．この遊離型テストステロンは，前立腺癌や精腺，肝などの標的器官に取り込まれて，5α-reductaseによりジヒドロテストステロンに変換されてアンドロゲン作用を示す．テストステロンとジヒドロテストステロンは，アンドロゲンレセプターに結合して標的遺伝子の機能を発現する．以上のことから血中テストステロン値の評価は，男性の性腺機能評価として不可欠のもの言える．現在，わが国では，主に総テストステロンもしくは遊離テストステロン値による評価が行われており，両値は日常臨床において病的な性腺機能下症や亢進症の診断にきわめて有用であることが実証されている．しかしながら，これらの測定値が男性ホルモンとしての生物活性をもっとも鋭敏に反映する測定値であるか否かについては必ずしも明確な国際的コンセンサスが得られておらず，欧米を中心に両値に代わる種々の測定指標が提唱されている．本稿ではテストステロン測定に関する現状と問題点を解説すると同時に，最近，日本泌尿器学会が中心となって設定した総テストステロン値と遊離テストステロン測定値の日本人における基準値についても紹介する．

テストステロンの種々の測定指標について

血中テストステロンは約98％が，SHBG結合型(SHBG-T)およびアルブミンとの結合型(albumin-bound-testosterone；Alb-T)であり，残りわずか1～2％が遊離テストステロン(遊離T)として存在する．これらアルブミンと結合したテストステロン(Alb-T)，SHBGと結合したテストステロン(SHBG-T)，遊離Tの３者を合わせて総テストステロン(総T)と称している(図1)．アルブミンと結合したテストステロンは結合力が弱く，容易にアルブミンから遊離するため，遊離TとAlb-Tがアンドロゲンとしての実際の生物活性を発揮すると考えられており，そのため遊離TとAlb-Tを合わせたものをbioavailable testosterone(BAT)

* Measurement of androgen concentration : current evaluation and problems.

** Toshihiko YANASE, M.D.: 九州大学大学院医学研究院病態制御内科〔〒812-8582 福岡市東区馬出3-1-1〕; Department of Medicine and Bioregulatory Science, Graduate School of Medical Science, Kyushu University, Fukuoka 812-8582, JAPAN

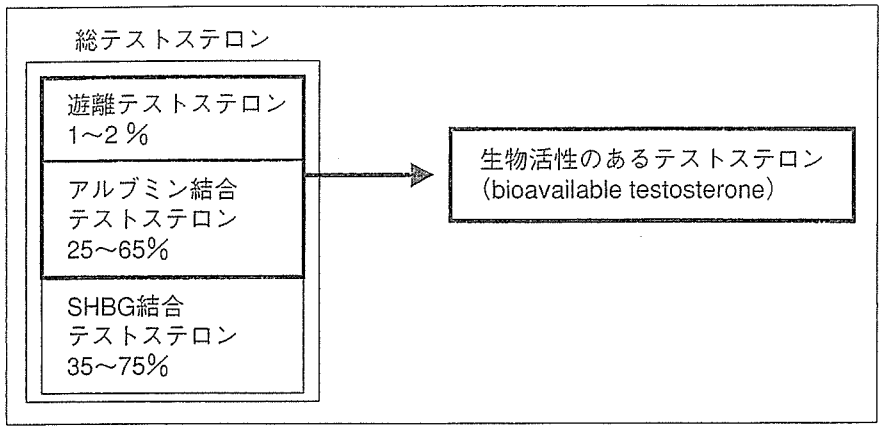

図1　血中でのテストステロンの存在様式

と呼んでいる[1)~3)]．国際的にはこのBATの測定が生物活性をもっとも正確に反映する指標として推奨されているが，SHBG結合型Tと非結合型Tの分画のために硫安沈降法，透析法，カラム法などの種々の煩雑な検体操作を要するため，少なくともわが国では日常臨床で用いられるまでには至っていない．

また，総T値，SHBG値，albumin値から算出するcalculated bioavailable testosterone[4)5)]をBATの代用とする方法も提唱されている．Calculated BATはhttp://www.issam.ch/freetesto.htmのweb siteのFree & Bioavailable Testosterone Calculatorを用いるとalbumin, SHBG, 総Tの値を入れるだけで算出されるが，残念ながらSHBGの測定はわが国では性腺機能検査としての保険適応がなく付加的経費がかかる点が難点である．

わが国では総T値ならびに遊離T値の測定は主にDPC社の固相法測定キットを用いて測定されている[6)]．ここでは遊離T測定RIAキットの測定原理について簡単に概説する．本キットのトレーサーは，ヨウ化テストステロン誘導体(ヨウ化ヒスタミン化ヒドロキシテストステロン)であり，誘導体であるためにSHBGあるいはアルブミンと結合しているテストステロンと置換することはなく，検体中にある非結合型(遊離)Tとヨウ化ヒスタミン化ヒドロキシテストステロンのみが競合して，固相T抗体と結合する．一方で固相T抗体も，Tに対する親和性がアルブミンやSHBGより低いものを用いているため，結合型Tと結合しないよう工夫されている．以上のことから原理的に検体中の遊離Tのみを主に認識する簡易なRIA系として使用されているが，結合型と非結合型の厳密な分画操作を伴わない簡易測定系であるため標準的測定法として国際的に評価されるまでには至っていない．しかしながら近年，calculated BATとBAT, calculated遊離Tと遊離Tがそれぞれ良好な相関性を示すことが報告され，またcalculated BATとDPCキットで測定された遊離Tの間には良好な相関が認められることも確認されている[7)8)]．よって，より正確な測定指標としてBATの測定やcalculated BATの算出が可能な限り望まれるとしても，現行の遊離T値の測定はその簡便性から，BATの測定に代替し得る測定指標として日常臨床で有用と考えられる．最近クローズアップされてきている男性更年期障害[9)]の診断指針の作成上の観点からも，わが国ではこの遊離T値や総T値の臨床上の有用性を見直し，積極的に活用する方向で再検討されている．そのためには，既存の基準値に比べ，より精度の高い信頼できる日本人男性の血中総T値と遊離T値の基準値の設定が必要である．最近，このような背景を受けて日本泌尿器学会が中心となり，測定条件等を厳密に検討した上での両値の日本人男性における基準値が設定されたので以下に紹介する[10)]．

日本人男性の総T値，遊離T値の基準値設定

健常に日常生活を営んでいる年齢20歳から77歳の男性1,143人を対象とし日本人成人男子の血清総Tおよび遊離Tの基準値設定をDPC・テストステロンキット〔(株)三菱化学ヤトロン〕，

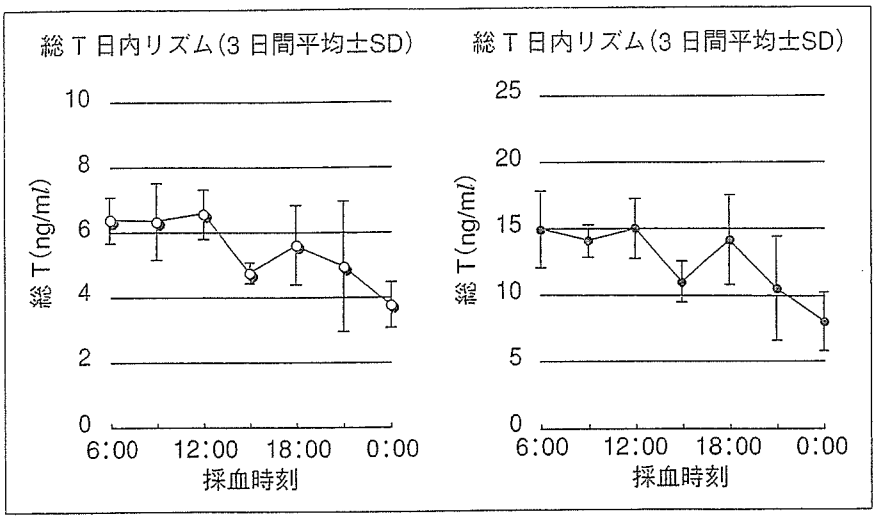

図2 総T，遊離T日内リズム

総T，遊離Tともに日内リズムを認め，挙動は一致していた．午前中は高値で比較的安定し，午後低下し，その後上昇するものの，夕～深夜にかけて低下し，深夜に最低値を示した．

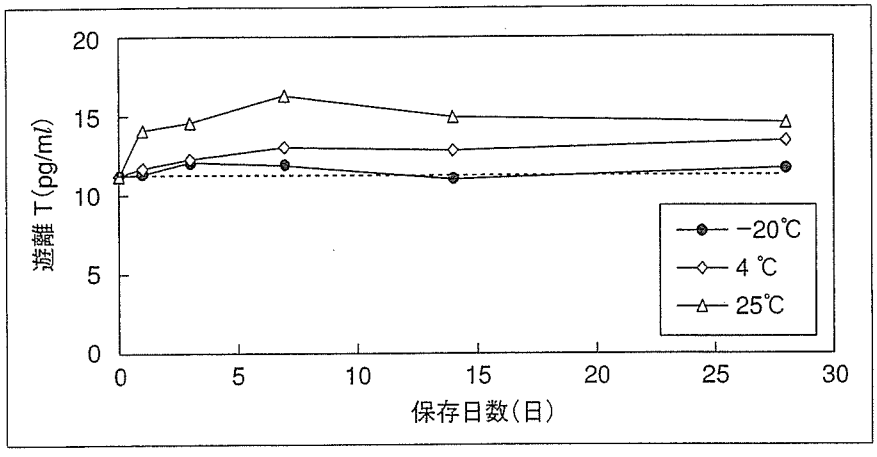

図3 遊離T保存安定性試験

遊離Tは，血清分離後の保存温度4℃，25℃では約7日後まで上昇し，30日後まで上昇した値で推移した．−20℃保存では，30日後まで値の変化はなかった．

DPC・フリーテストステロンキット〔(株)三菱化学ヤトロン〕を用いて行った[9]．

1．総T値および遊離T値の日内リズム

3名の健常男子ボランティア3名を対象にした結果によれば，総T値および遊離T値には平行に推移する顕著な日内リズムが存在する(図2)[9]．両者ともに午前中に比較的安定に高値を持続した後，午後にかけて低下し，就寝前にもっとも低値となった．これらのことから，採血時間は，高値で安定な結果を生む午前中に実施するべき考えられる．

2．保存安定性

血清分離後の保存安定性については，総Tは4℃，室温，および37℃保存で少なくとも18時間は安定である．一方，遊離Tは室温6時間放置で高値化し，その後30日間高値を持続したが，−20℃保存では30日間安定であった(図3)．また，両項目とも6時間内で実施した凍結融解の検討では5回まではその影響を認めなかった[9]．T自体は熱に安定であり，実際総Tに変化がないことから，室温放置下では結合型TからTが解離するに遊離T値が上昇するものと考えられた．したがって，採血後は，遊離Tは不安定であるため血清分離後，すみやかに凍結保存する必要がある．総T値の測定のために凍結保存の必要はなく，約3日以内に測定すれば4℃での保存

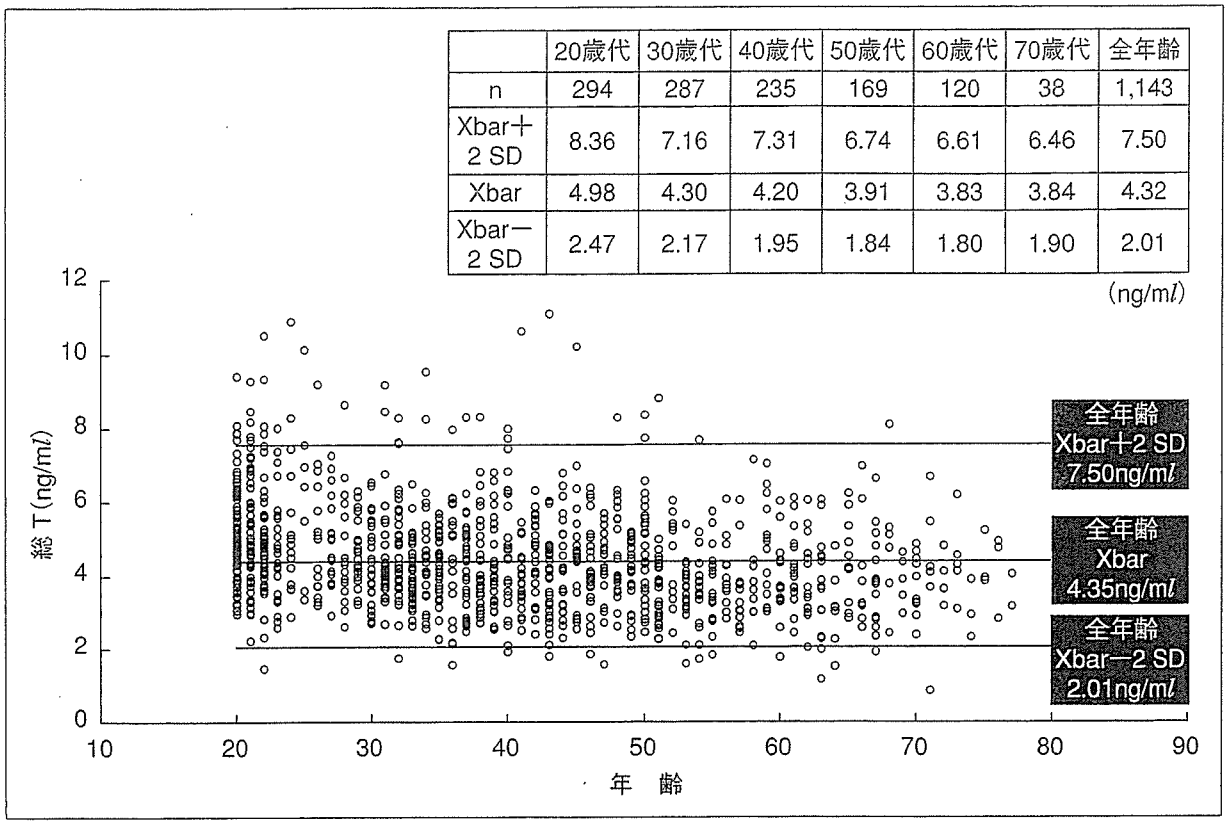

図4　総T基準値

総Tは，20～77歳の全例を一括統計処理し，Xbar±2 SDを基準値とした．上限値(Xbar＋2SD)：7.50ng/ml平均値(Xbar)：4.35ng/ml，下限値(Xbar－2 SD)：2.01ng/mlであった．

で十分である．一方，遊離T値の測定には凍結保存が必要である．

3．基準値設定

1，2の結果から，採血は午前中に実施し，分離した血清検体は測定まで－20℃保存した，総T値は加齢とともに若干低下傾向を示したが，50歳代以降ではほとんど変化がなく一定に推移した(図4)．総Tの基準値は加齢の影響が小さかったことから全データを一括して2.01～7.50ng/ml(平均±2 SD)と設定した．一方，遊離Tは年齢との間に強い相関性を示し加齢とともに低下した(図5)．その相関はy＝－0.161x＋20.7(r＝－0.521)で，低下速度は10年間で－1.61pg/ml(－9.2%)であった．このため遊離Tは10歳ごとの年齢階層別基準値平均値±2 SD)として設定した．20歳代は8.5～27.9pg/ml，30歳代は7.6～23.1pg/ml，40歳代は7.7～21.6pg/ml，50歳代は6.9～18.4pg/ml，60歳代は5.4～16.7pg/ml，70歳代は4.5～13.8pg/mlと設定した[10]．

20歳代から70歳代にかけて基準上限値は27.9pg/mlから13.8pg/mlへと大幅に低下するのに対し，下限値は8.5pg/mlから4.5pg/mlとわずかな低下であった．その下限値は加齢でほとんど変化がないことから「男性らしさ」を維持するには最低限，5 pg/ml程度の血中濃度を必要とすると考えられるが，逆にこれ以下の低下は病的とも判定できる．

おわりに

The International Society for the Study of the Aging male(ISSAM)の定義によれば，男子更年期障害は「加齢に伴う血中男性ホルモンの低下に基づく生化学的な症候群」と定義され[11]，欧米ではpartial androgen deficiency(declining) in aging male(PADAM)あるいはlate-onset hypogonadism(LOH)と称されている．しかしながら，男子更年期障害に該当すると考えられるすべての患者群において必ずしも低テストステロン血症が認められるわけではないことも指摘されており[12]，このことが診断ガイドライン作成上の大